Conf-820238--5

LBL-14059

Lawrence Berkeley Laboratory
UNIVERSITY OF CALIFORNIA

Presented at the MARIA Heavy Ion Workshop, Banff, Alberta, Canada, February 22-26, 1982

THE TARGET NUCLEUS IN RELATIVISTIC NUCLEAR COLLISIONS

Hans H. Gutbrod, A.I. Warwick, and H. Wieman

March 1982

NUCLEAR SCIENCE DIVISION

MASTER

DISTRIBUTION OF THIS DOCUMENT IS UNLIMITED

Prepared for the U.S. Department of Energy under Contract DE-AC03-76SF00098

DISCLAIMER

LBL-14059

THE TARGET NUCLEUS IN RELATIVISTIC NUCLEAR COLLISIONS*

Hans H. Gutbrod, A.I. Warwick, and H. Wieman
Gesellschaft für Schwerionenforschung
D-6100 Darmstadt, West Germany
and
Nuclear Science Division, Lawrence Berkeley Laboratory
University of California, Berkeley, CA 94720

INTRODUCTION

Since the earliest Bevalac experiments one of the main goals in the field of relativistic nuclear collisions is the determination of the equation of state of nuclear matter, particularly at densities much larger than the nuclear density. Over this period attempts have been made to observe, in relativistic nuclear collisions, collective phenomena that would justify terms like density, pressure, temperature, and phase transition: in other words, terms associated with states in equilibrium.

In 1976, the nuclear *fireball model*[1] was formulated, predicting not only the emission of nucleons but also the production of clusters like deuterons, tritons, etc., which were assumed to be in chemical equilibrium. The geometry for a given impact parameter defined how many particles would interact with one another, thus being called the participants, and how many particles in each nucleus would miss a collision, thus being called the spectators. For small projectile and large target nuclei and rather central collision it means that the target would sweep out a cylinder-like part of the target nucleus and form with it a nuclear or hadronic fireball. Since the geometry defines the number of participants in the fireball, its temperature and velocity are well defined and only in the cluster production is there a parametrization of the freeze out density at which the chemical activity stops.

In the original paper[1] it was pointed out that the nuclear fireball geometry should fail for central collisions and a target explosion was suggested instead. Despite a systematic discrepancy with the data,[2] this model has been and is still used extensively today. It is probably the simplicity of this model with the full thermodynamical and chemical equilibrium features that attracts theorists to play with it without huge computer costs or time-consuming efforts.[3] This systematic discrepancy with the data,[2] however, points out that the apparent temperature in the data is higher than calculated in the clear-cut geometry. Through these and other data the geometric assumption of the fire-models and the total participant-spectator picture are challenged.

*This work was supported in part by the Director, Office of Energy Research, Division of Nuclear Physics of the Office of High Energy and Nuclear Physics of the U.S. Department of Energy under Contract DE-AC03-76SF00098.

The only model with a direct link to the equation of state of nuclear matter is the hydrodynamical model,[4] which treats the nuclear collision as that of two liquids. A local thermal equilibrium is always established. This model is based on small mean free paths of the nuclear constituents. A somewhat orthogonal view is taken in the intranuclear cascade model,[5] where nuclear collisions are treated as cascades of nucleon-nucleon collisions with cross sections taken from nucleon-nucleon scattering data.

Both models predict, in a central collision, a fast energy dissipation in the early diving stage of the projectile into the target nucleus. In the final state both models show total incident energy largely dispersed over the whole target nucleus. In a quantitative comparison with the data for the Intranuclear Cascade Calculations, however, the 90° double differential cross section seems to be flatter than the calculated one. If the slope is reflecting the temperature in the system then the data are having apparently a higher temperature than the cascade would predict.

This report will suggest and discuss a picture of the reaction mechanism where the light projectile (e.g. Ne) "gets stopped" very early in the large target nucleus (e.g. Au or U) forming a small fireball at approximately half the beam rapidity, which decays inside the target nucleus, heating it up and causing the whole system to expand. The expansion cools the system and big clusters can condense out if the total energy and thus entropy in the system is not too high to prevent it.

Such a qualitative picture of a reaction mechanism emerges when we consider the information obtained about relativistic nuclear collisions from measurements of the remnants of a large target nucleus struck by a smaller projectile (Ne + Au) and relate it to the complementary information from earlier measurements[2] of fast light reaction products. In this sense we are also reviving aspects of earlier proton-nucleus measurements[6] and comparing them to more complex correlation data.

EXPERIMENTS

Most of the data discussed here have been collected with the system depicted in fig. 1. It consists of three subsystems, the vacuum-scattering chamber with a diameter of 1 meter and wall thickness of 3 mm of Al, the 80-fold plastic scintillator array around the scattering chamber, and the Plastic Wall covering the forward angles of 2.5° to 9°. Inside the scattering chamber in earlier measurements of π^+, p, d, t data[2] a Si-Ge telescope was used. Later for the measurements of very slow fragments[7] a single gas ionization chamber with Si-E detectors and an array of 5 Si detectors in coincidence were used. Finally, the pictured system of parallel-plate avalanche counters, silicon walls, and 4 ΔE-E telescopes was mounted, a total of 48 telescopes inside the chamber[8]. This enabled us to study all the various correlations between the slow fragments and between the slow and fast fragments, as measured in the 80 scintillator multiplicity array outside the vacuum chamber. Special efforts were made to achieve the lowest possible energy cutoff for the heavy fragments. This was done by building start detectors for the TOF system with a thickness of only 150 $\mu g\ cm^{-2}$. The multiplicity array yields data on the charged particle multiplicity associated with a fragment measured inside the scattering chamber. Thus the charged

particle multiplicity associated with the trigger fragment is a characterization of the event. The energy of the charged particles has to be larger than 25 MeV/n in order to penetrate the 3 mm Al chamber wall and fire the plastic scintillator.

STOPPING OF THE PROJECTILE

A reaction can be crudely described by the projectile's energy loss. A compound nucleus reaction shows total momentum and full energy transfer. Other reactions might depend only on the velocity of the passive projectile asymptotically limited by the speed of light.

At low bombarding energies around 5 MeV/u the reaction mechanisms are fairly well established and can be selected by the choice of the proper fragment mass. Over a large range of incident energies, however, the mechanism for a specific fragment emission might change its character completely.

At low energies around 5 MeV/u the compound nucleus formation is the reaction where the projectile "gets stopped" in the target nucleus forming a new system with a specific excitation energy and angular momentum. This system decays via evaporation and/or fission. For ^{4}He + U the compound nucleus or the target nucleus decay predominantly via fission and this mechanism has been studied extensively over a large range of incident energies, for 5 MeV/u up to 2 GeV/u.[7] At low energies two fission channels are operating, in a central collision the compound nucleus dominantly decaying via fission and for very peripheral collisions the U target nucleus undergoing fission after being excited in inelastic collisions (e.g. Coulomb fission). At energies beyond 15 MeV/u the fusion-fission in a central collision decreases until at high incident energies only the peripheral reaction can proceed through the fission channel. (Thus, if one wants to study the central collisions over a large range of energies, some other channel has to be found that is clearly related to a small impact parameter.) It is then of interst to find out what happens to the target nucleus in a central collision at high energies.

Looking to the opposite end of the mass spectrum of emitted particles one can study the proton and deuteron emission in a reaction. This has been done extensively since 1975 in single particle inclusive measurements. More recently, coincidence experiments have directly measured the multiplicities of these light fragments.[2] The multiplicity can give information on the amount of energy dissipated inside the target nucleus.

Using the results of an experiment,[2] obtained with the facility described, the light particle emission will be discussed first to find out how it agrees with the participant spectator idea mentioned in the introduction.

The charged particle multiplicity associated with the observation of a proton at 90° is shown in Fig. 2 plotted versus the average number of participants, as measured in various projectile-target combinations.[2] As the incident energy is increased the charged particle multiplicity is increasing way beyond the participant number. What is measured in this experiment is more than the participants, and a source other than the fireball has to be found to produce many particles beyond 25 MeV kinetic energy (proton

equivalent). If one looks in a different way at the charged particle multiplicity associated with the 90° proton, namely as a function of total incident kinetic energy for a heavy target, then, as shown in Fig. 3, one observes a continuous rise up to 42 GeV. Even when changing the trigger particle from a proton to a deuteron or triton or a slow fragment like C, O, or Ne, the total kinetic energy is determining the charged particle multiplicity as shown in Fig. 4 for 4 and 8 GeV ^{4}He and ^{20}Ne on Au.[7] Such a strong dependence, independent of projectile size, rules out totally the simple geometry of the fireball[1] and its related models,[3] which had assumed a clean-cut geometry. This rise of the associated charged particle multiplicity as a function of incident total energy leads one to conclude that the target nucleus gets blown apart more and more the higher the incident energy.

Another important piece of information on the reaction mechanism is contained in the single particle inclusive spectra of high multiplicity events.[9] In fig. 5 it is shown that at 2.1 GeV/u ^{20}Ne + U apparent temperatures of up to 150 MeV have been observed, much higher than the fireball model predictions of ∿100 MeV. For a thermal system this is only possible if the available energy is dissipated among fewer constituents in the fireball, i.e. if the number of degrees of freedom is much smaller.

Thus we have made two observations seemingly contradicting each other.

a) The total kinetic energy of the projectile determines how many fast particles can be observed and one concludes that more nucleons participate in the collision process than is predicted by the fire models.

b) The slope of the spectra indicate a higher temperature than calculated in the participant-spectator geometry and with the fireball chemistry. One wants to conclude that the emitting system is smaller than the fireball.

One can resolve that puzzle by considering b) to be the experimental proof for a primary reaction zone (hot spot) in the heavy target nucleus where the projectile interacts with an equal number of nucleons. From this primary reaction some particles are emitted, thermal and/or nonthermal, into the cold remainder of the target nucleus, some penetrating to the outside. A large fraction of these emitted particles can reach a detector at large angles without having to penetrate the cold target residue and exhibit the features of emission from a symmetric nucleon-nucleon system showing a high temperature. At forward angles, for small impact parameters, most emerging particles go through the rest of the target nucleus, being attenuated according to their mean free path, and reach the detector with less energy than they started out with. The energy loss of the particles emitted into the cold target remnant heats it up and leads to the tremendous increase of charged particle multiplicity due to cascading effects. Some clusters like deuterons, tritons, or ^{3}He can be emitted if nucleons are close in momentum space and interacting with a mean field or a third body to get rid of the excess energy after coalescence[10].

If equilibrium is established in the hot zone, a chemical potential calculation[1,11] will be appropriate to describe the formation of clusters. Due to the high temperature of the hot spot the cross sections would fall off with increasing cluster mass and the binding energies (particularly for alpha particles) would have less influence on the cluster formation than at lower temperatures.

EXPANSION AND COOLING

This section focuses on the old question from high energy proton-nucleus reactions[6] "why are there so many low energy ^{4}He particles and so few ^{3}He, why is the cross section at higher fragment energies larger for ^{3}He than for ^{4}He[1]?[11] (Fig. 6,7) For a long time the ^{4}He emission at low ^{4}He energies was considered to come from reactions with low deposition energies while the ^{3}He emission was to come from higher deposition energies.[6] It was found, however, that this is not true and that ^{4}He was also produced in the type of event characterized by a high associated charged particle multiplicity (see fig. 8). Thus, one can visualize these ^{3}He and ^{4}He being emitted from the same kind of events where proton spectra tell of temperatures of up to the limiting temperature of 150 MeV.

One explanation for this ^{3}He-^{4}He puzzle can be that the temperature is changing with time, due to an expanding system. At the beginning the hot spot emits p, d, t, and more ^{3}He than ^{4}He due to the very high temperature. As the target explosion makes the nuclear system expand, it cools, until it reaches temperatures low enough that the strong binding energy of ^{4}He favors its formation over that of ^{3}He. In this picture the large cross section for ^{4}He production originates from a late state where nuclear condensation dominates.

Following the idea of condensation into clusters we next address the question of the production mechanism of heavier clusters, which have been found to originate in violent collisions (Fig. 4).

SLOW HEAVY FRAGMENTS

The double differential cross sections at 90° for fragment masses between 28 and 31 amu are shown for all reactions studied in Fig. 9. These spectra depict peaked distributions where the peak energy was usually associated with the Coulomb force of the emitting system and the slope with its temperature. For all these various reactions there is astonishingly little change in shape. This is more evident when going to even heavier fragments of the mass range of 120 to 140, i.e., 60 to 80 masses away from the target-nucleus (Fig. 10). Their spectra are nearly identical in shape and remind one of the slope of 8 MeV measured in projectile fragmentation at 0°[12]. From single particle inclusive measurements one cannot learn how the fragment masses from various mass regions are associated with each other, an essential question in the study of the reaction mechanism involved. For such an investigation these slow fragments with energies of around 0.5 to 5 MeV/u and masses from 6 to 40 amu are subject of the following discussion:

a) Are these fragments produced in an evaporation/fission-like process with acceleration due to the Coulomb field of a second body?

b) Are these fragments from a shattered target nucleus leaving many heavy fragments behind?

c) Or are these fragments condensation products from a nearly totally vaporized target nucleus?

In a recent experiment[8] with the system shown in fig. 1, it was clearly established that light fragments with masses from 10 to 30 were not produced via a fission-like process, leaving behind a large residue. Figure 11 shows the associated charged particle multiplicity with the detection of a fragment mass. The majority of light mass fragments 20-40 have a different multiplicity from those of high masses, which otherwise could have been considered partner nuclei to the lighter masses in a fission-like decay. Thus the Coulomb peak in the light fragment spectra must refer to the Coulomb force from a many body sytem and explanation a) can be ruled out as the dominant process.

How many of these light fragments are produced in these reactions is shown in Fig. 12 (for the average event). The multiplicity of finding a given fragment mass in an event in which a trigger fragment of A = 20-40 is emitted is plotted for two different energies. It is very low for associated fragments beyond a Z of 4, i.e., there are very few massive fragments, on the average, associated with a mass 20-40 fragment. Dominantly these fragments of A = 20-40 are associated with ^{4}He, Li particles. One can assume that there is also a large multiplicity of slow protons, deuterons, and tritons associated with these fragments.

For the bombarding energies between 250 MeV/u and 2.1 GeV/u one can state that the light fragment production is associated with a large multiplicity of fast charged particles, a substantial multiplicity of (H), He, Li fragments and only a very small multiplicity of heavy fragments. (At low bombarding energies like 86 MeV/u this is not true any longer. There the disintegration of the target nucleus is much less violent and breakup into dominantly several large fragment masses has been observed as a substantial reaction channel[13].) Table I gives an account for the associated masses when a fragment with mass 20-40 is observed. From earlier p-nucleus studies[6] the ratio of ^{4}He cross section to that of slow protons below an energy of 25 MeV was extracted and from neutron measurements[14] the number of neutrons was deduced as approximately four times the number of protons. This yields roughly 24 neutrons and 6 protons at energies below 25 MeV. One observes that at 2.1 GeV/u the whole target mass has been accounted for, i.e., the incident Ne projectile caused the explosion of the Au nucleus supporting c) and b) can be ruled out also at high bombarding energies (2.1 GeV/u Ne).

At 8 GeV total incident energy it was found[7] that collisions leading to an emission of a slow fragment like C had the highest charged particle multiplicity, therefore coming from the most central collisions. Figure 13 shows that at total incident energies of 20 and 42 GeV, this is no longer true. In there cases the slow fragment emission is associated with a 50% lower charged particle multiplicity than are protons[2] emitted to 90° pointing out that there are more energetic explosions than the ones that lead to a mass 20-40 fragment emission.

CONDENSATION

The reported data on ^3He-^4He productions, on the slow fragment emissions, their associated slow and fast charged particle multiplicities with their dependence on incident energy, all that has to be kept in mind when the total yield curve is compared for masses from 4 to 30. In fig. 14 this mass yield curve is plotted for the systems investigated in this experiment. Note the difference in the cross section of 1.4b to 13b when extrapolated values from ref. 15) are compared with data covering the low-energy part of the spectrum inaccessible to the high-energy data. To describe these data simple fireball-yield curves[16] have been plotted with the temperature as a search parameter (fig. 14). It is found that the light particle yield dominated by high-energy particles is best described with a temperature of 140 MeV, whereas the fragment yield of slow particles is best described by a temperature of 18-20 MeV.

An alternative description, as already brought up in the ^3He-^4He discussion, is that of condensation. As the word evaporation is inappropriate for the emission of the ^4He in a reaction leading to total disintegration of the nucleus and since the heavier fragments (C,N,O) are from similar events as are the ^4He, it is inviting to assume the same production mechanism for both. Following the "theory of condensation and the critical point" by M.E. Fisher,[17] one can write down the probability to find a cluster of size A condensed out of a vapour to be:

$$\sigma_A \propto A^{-\tau} \quad \text{with } \tau \text{ typically } 2.33.$$

In Fig. 15 the cross sections for fragment emission are plotted and compared with such a prediction. It is astonishing how closely such a simple formula describes the data. It must be mentioned that the Purdue-Fermilab collaboration[18] has brought our attention to this power law, describing the fragment cross sections of high energy proton nucleus interactions. It is our intention to consider this power law to be indicative of the liquid-vapor phase transition, as described by Fisher.[17] The best fit seems to be for $\tau \approx 2.6$. As Fisher points out, the condensation can only take place if the critical point is reached where the entropy in the vapor is balanced by the surface tension of the droplet to be formed. It is our understanding of the high-energy data that beyond 20 GeV incident total energy the nuclear vapor can be heated up to higher temperatures so that the system does not cool enough to reach that condensation point. Only in less central collisions at 1.05 and 2.1 GeV/u is this possible, thus changing the character of a heavy fragment trigger from a very central one to a more peripheral one as one increases the incident total energy.

CONCLUSION

Due to an event characterization via the associated charged particle multiplicity it has been shown that several of the older model pictures, invented to understand single particle inclusive high-energy proton-nucleus data, are not adequate to describe correlation data. It was shown that the participant-spectator model needs revision and that a quick stopping in a small volume in the target nucleus is indicated. Furthermore, the whole nucleus is made to explode if the incident energy is high enough. The

^4He-^3He yields point towards an early and a late production of helium with a strong favoring of α-condensation at low temperatures[19] (fig. 16). The vapor-to-cluster condensation theory is astonishingly good at describing the observed mass yield.

This report is strongly based on the work of many collaborators[1,2,7,8,10]. We appreciate especially the support of A.M. Poskanzer, H.G. Ritter, and F. Weik from LBL and GSI and of S. Kaufman, E. Steinberg, and B. Wilkins from ANL. One of us (H.H.G.) enjoyed very much the hospitality at the Maria Heavy Ion Workshop in Alberta. This work was supported in part by the Director, Office of Energy Research, Division of Nuclear Physics of the Office of High Energy and Nuclear Physics of the U.S. Department of Energy under Contract DE-AC03-76SF00098.

REFERENCES

1) G.D. Westfall, J. Gosset, P.J. Johansen, A.M. Poskanzer, W.G. Meyer, H.H. Gutbrod, A. Sandoval, and R. Stock, Phys. Rev. Lett. 37, 1202 (1976).
J. Gosset, H.H. Gutbrod, W.G. Meyer, A.M. Poskanzer, A. Sandoval, and G.D. Westfall, Phys. Rev. C16, 629 (1977).

2) A. Sandoval, H.H. Gutbrod, W.G. Meyer, A.M. Poskanzer, R. Stock, J. Gosset, J.-C. Jourdain, C.H. King, G. King, Ch. Lukner, Nguyen Van Sen, G.D. Westfall, and K.L. Wolf, Phys. Rev. C21, 1321 (1980).

3) W.D. Myers, Nucl. Phys. A296, 177 (1978).
J. Gosset, J.I. Kapusta, and G.D. Westfall, Phys. Rev. C18, 844 (1978).

4) A.A. Amsden, F.H. Harlow, and J.R. Nix, Phys. Rev. C15, 2059 (1977).
A.A. Amsden, A.S. Goldhaber, F.H. Harlow, and J.R. Nix, Phys. Rev. C17, 2080 (1978).
H. Stöcker, W. Greiner, and W. Scheid, Z. Physik A286, 121 (1978).
H. Stöcker, J.A. Maruhn, and W. Greiner, Z. Physik A293, 173 (1979).

5) Y. Yariv and Z. Fraenkel, Phys. Rev. C20, 2227 (1979).
Y. Yariv and Z. Fraenkel, Phys. Rev. C24, 488 (1981).

6) e.g. A.M. Poskanzer, G.W. Butler, and E.K. Hyde, Phys. Rev. C3, 882 (1971).
A.M. Zebelman, A.M. Poskanzer, J.D. Bowman, R.G. Sextro, V.E. Viola, Phys. Rev. C11, 1280 (1975).

7) W.G. Meyer, H.H. Gutbrod, Ch. Lukner, and A. Sandoval, Phys. Rev. C22, 179 (1980).

8) ANL-GSI-LBL Coll. Experiment 489H at the Bevalac.

9) H.H. Gutbrod, Proc. of the Hakone Seminar, July 1980, p. 93.

10) H.H. Gutbrod, A. Sandoval, P.J. Johansen, A.M. Poskanzer, J. Gosset, W.G. Meyer, G.D. Westfall, and R. Stock, Phys. Rev. Lett. 37, 667 (1976).

11) A. Mekjian, Phys. Rev. Lett. 38, 640 (1977); and Phys. Rev. C17, 1051 (1978).

12) K. Van Bibber, D.L. Hendrie, D.K. Scott, H.H. Wieman, L.S. Schroeder, J.V. Geaga, S.A. Chessin, R. Treuhaft, J.Y. Grossiord, J.O. Rasmussen, and C.Y. Wong, Phys. Rev. Lett. 43, 840 (1979).

13) W.F.J. Müller, et al., Hirschegg X (1982) and I. Otterlund, private communications, 1982.

14) W. Schimmerling, J.W. Kast, D. Ortendahl, R. Madey, R.A. Cecil, B.D. Anderson, and A.R. Baldwin, Phys. Rev. Lett. 43, 1985 (1979).

15) S. Nagamiya, M.C. Lemaire, E. Moeller, S. Schnetzer, G. Shapiro, H. Steiner, and I. Tanihata, Phys. Rev. C24, 971 (1981).

16) G. Fai and J. Randrup, preprint LBL-13357 and private communications.
17) M.E. Fisher, Physics 3, 255 (1967).
18) A. Hirsch, et al. (1981) Asilomar Meeting, and R. Scharenberg, private communications.
19) P.R. Subramanian, L.P. Csernai, H. Stöcker, J.A. Maruhn, W. Greiner, and H. Kruse, J. Phys. G: Nucl. Phys. 7 (1981) L241; and L. Münchow and H. Schulz, Hirschegg X (1982).

TABLE I

MASS ACCOUNTING IN THE AVERAGE VIOLENT EVENT Ne + Au

Trigger Fragment: Mass 20 to 40 Associated Masses:	Beam Energy 400 MeV/u		2100 MeV/u	
Slow fragments $\sum_{A=4}^{40} \langle M_{slow} \rangle A$	44		39	
Fast charged part. $\langle M \rangle$	20	126	42	178
Fast neutrons	32		67	
Slow n (~24) and p (~6) below 25 MeV	~30		~30	

FIGURE CAPTIONS

1) Experimental setup[2,7,8] used to measure correlations among slow fragments and their associated fast particles.
2) Charged particle multiplicities associated with the detection of a 20-200 MeV proton at 90° in the lab system, plotted versus the average number of participants.
3) Charged particle multiplicity associated with the detection of a 20-200 MeV proton from the bombardment of a U target with p, ^{4}He, ^{20}Ne, ^{40}Ar beams plotted versus the full beam energy.
4) Charged particle multiplicity associated with the detection of low energy fragments with $3 < Z \leq 26$.
5) Double differential cross section of protons from high multiplicity reactions.
6) Hydrogen and helium spectra from 5 GeV proton-U collisions.
7) Helium spectra from 42 GeV Ne on U.
8) Multifold coincidence distribution of charged particles associated with the detection of π^{+}, p, ^{16}O, and 20 MeV ^{4}He at 90° lab.
9) Double differential cross section of mass 29-31 detected at 90°.
10) Double differential cross section of mass 120-140 detected at 90°.
11) Fast charged particle multifoldness as a function of the mass of the trigger particle.

12) Mean multiplicity of fragments with charge Z associated with a mass 20-40 fragment at ∿90° for Ne + Au. Also fragment cross sections scaled arbitrarily for comparison of Z dependence.
13) Average charged particle multiplicity associated with proton emission and with slow light fragment emission into 90° as a function of total projectile energy.
14) Mass yield curves for element emission compared to fireball calculations. The yield curve labeled 155 MeV is a calculation yielding absolute cross sections. The curves labeled 10-20-40 MeV are arbitrarily normalized.
15) Fragment yields compared to the power law $\sigma_A \propto A^{-\tau}$ (with τ varying from 2.33 to 3.2) of the general condensation model[16].
16) Schematic view of the time dependent change of the temperature in the reaction, feeding at different times different parts of the He spectra.

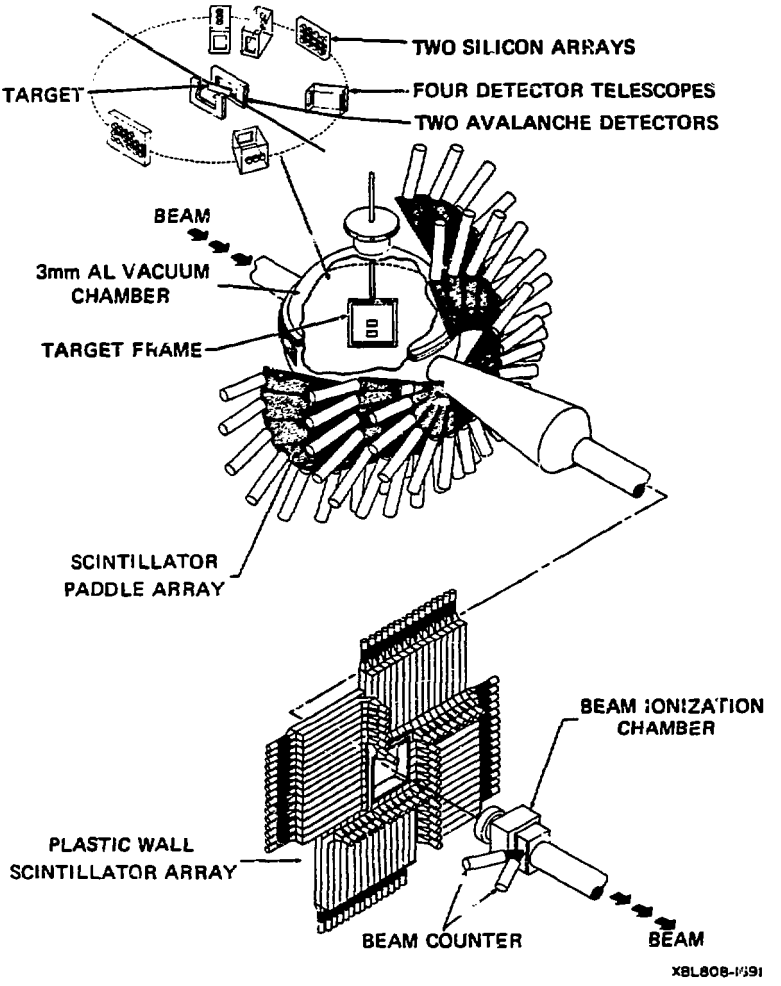
TWO SILICON ARRAYS
TARGET
FOUR DETECTOR TELESCOPES
TWO AVALANCHE DETECTORS
BEAM
3mm AL VACUUM CHAMBER
TARGET FRAME
SCINTILLATOR PADDLE ARRAY
BEAM IONIZATION CHAMBER
PLASTIC WALL SCINTILLATOR ARRAY
BEAM COUNTER
BEAM
XBL808-1491

Fig. 1

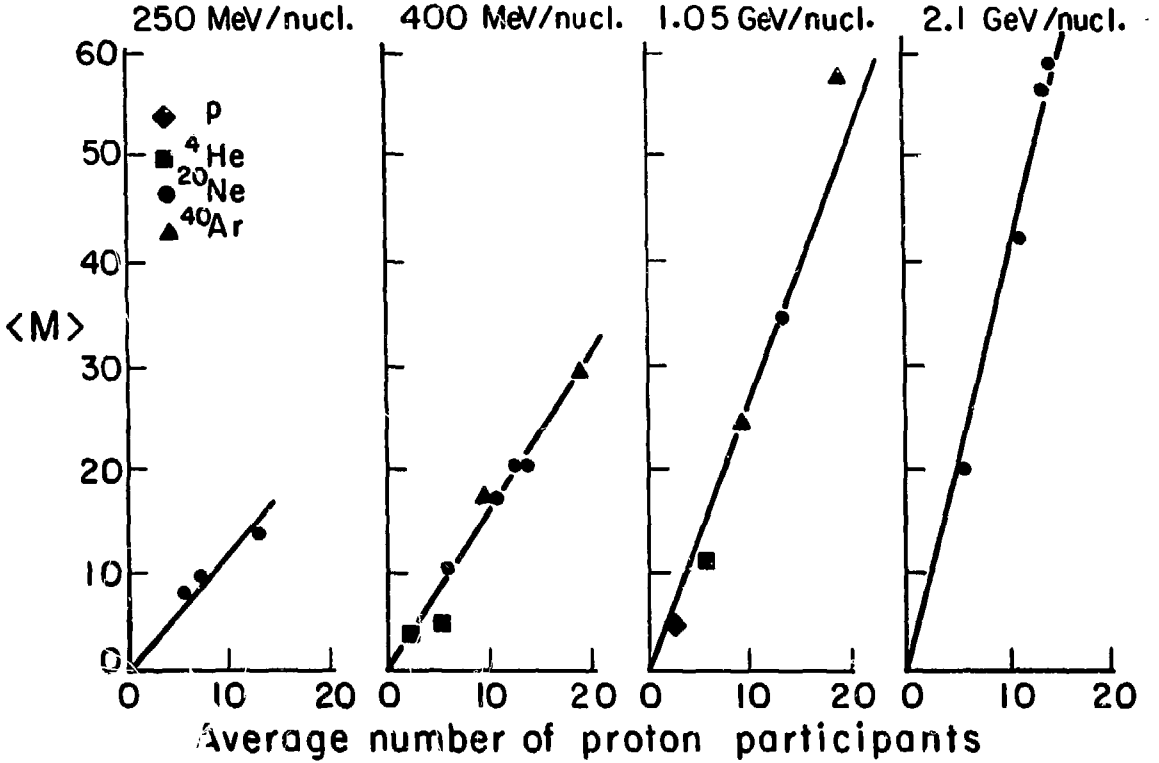

XBL 787-1322A

Fig. 2

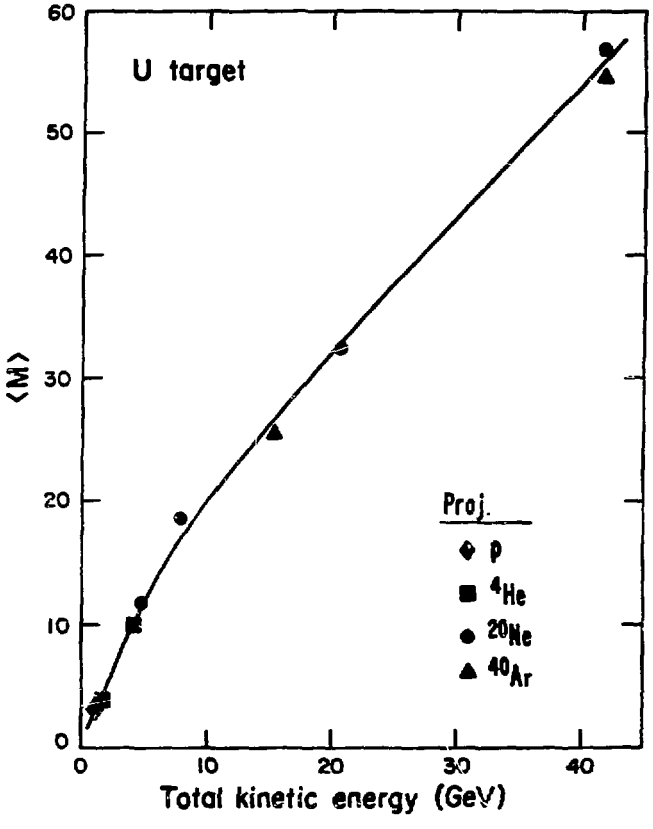

XBL 797 - 2054

Fig. 3

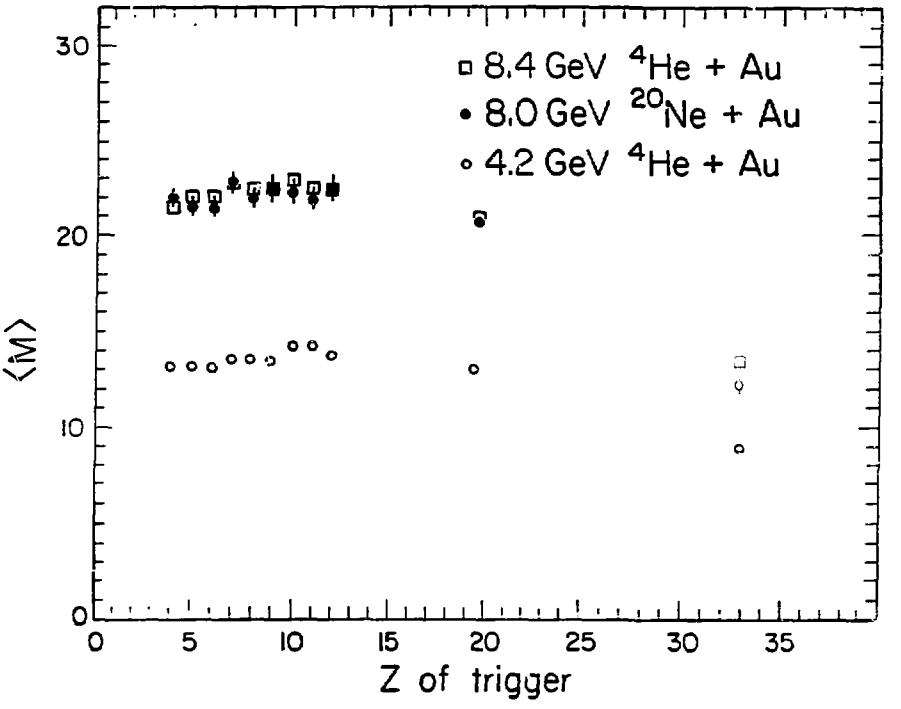

XBL 797-2135

Fig. 4

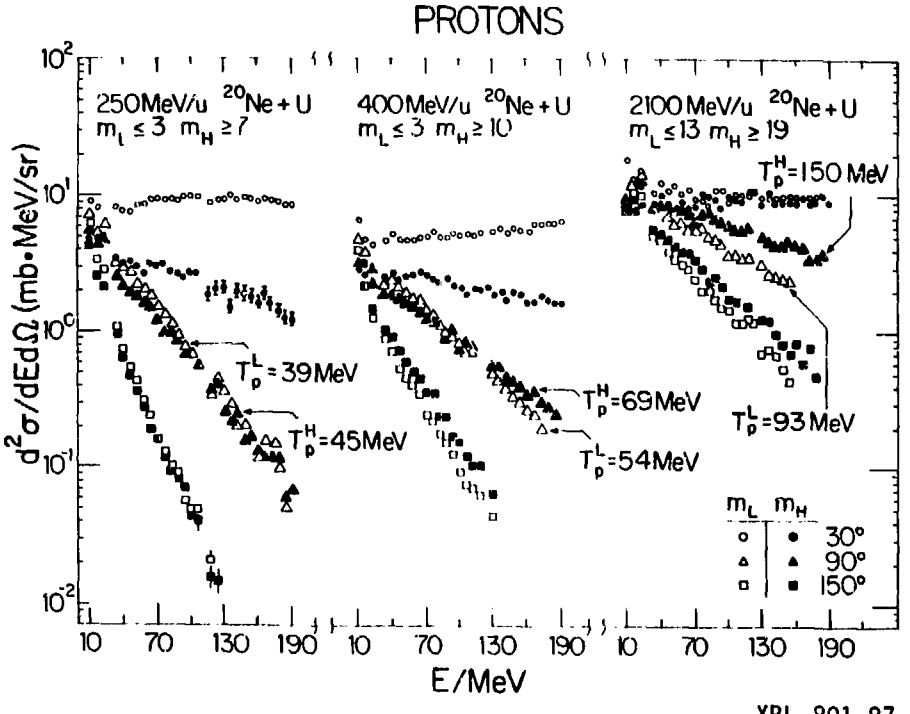
PROTONS
250MeV/u ^{20}Ne + U
$m_L \leq 3$ $m_H \geq 7$
400MeV/u ^{20}Ne + U
$m_L \leq 3$ $m_H \geq 10$
2100MeV/u ^{20}Ne + U
$m_L \leq 13$ $m_H \geq 19$
T_p^H=150 MeV
T_p^L=39MeV
T_p^H=45MeV
T_p^H=69MeV
T_p^L=54MeV
T_p^L=93MeV
m_L m_H
30°
90°
150°
$d^2\sigma/dEd\Omega$ (mb•MeV/sr)
E/MeV
XBL 801-87

Fig. 5

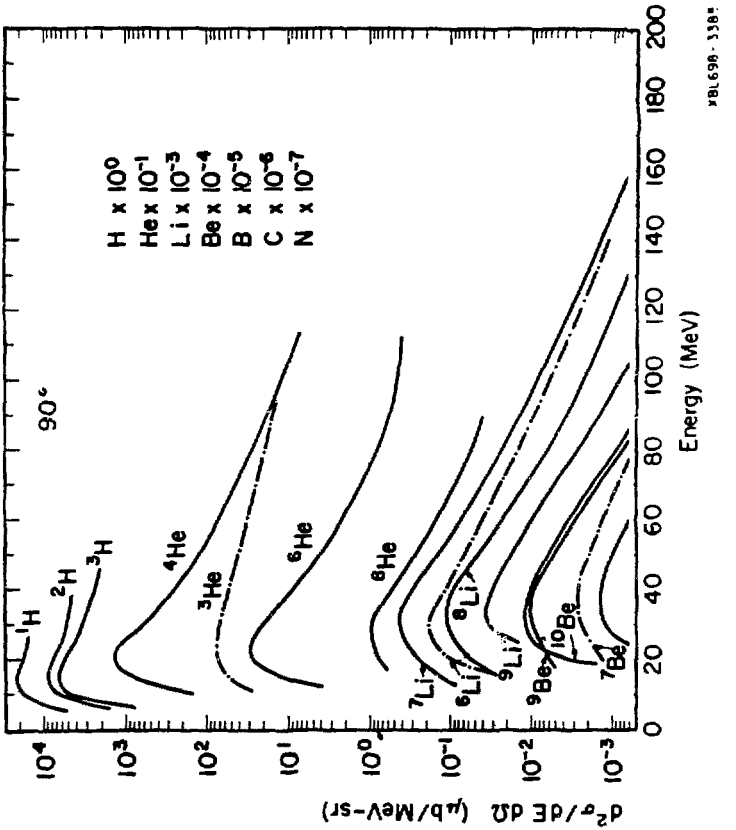
H x 10^0
He x 10^-1
Li x 10^-3
Be x 10^-4
B x 10^-5
C x 10^-6
N x 10^-7
90°
1H
2H
3H
4He
3He
6He
8He
7Li
6Li
8Li
9Li
9Be
10Be
7Be
d²σ/dE dΩ (μb/MeV-sr)
Energy (MeV)
XBL698-3385

Fig. 6

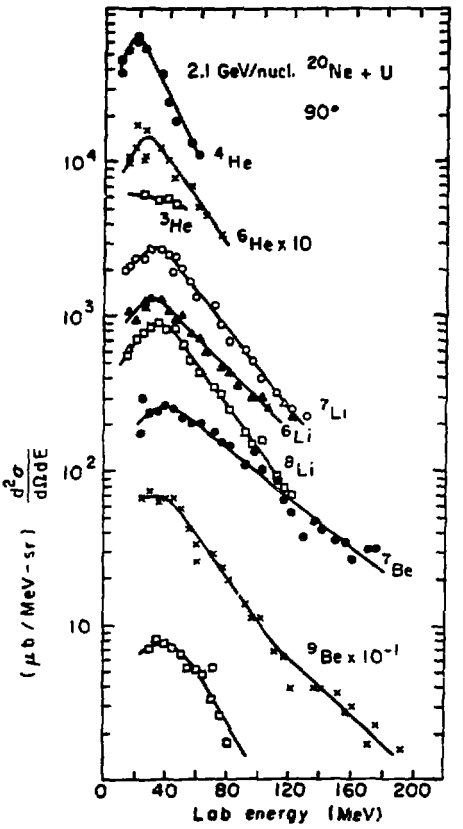

XBL 798-3795

Fig. 7

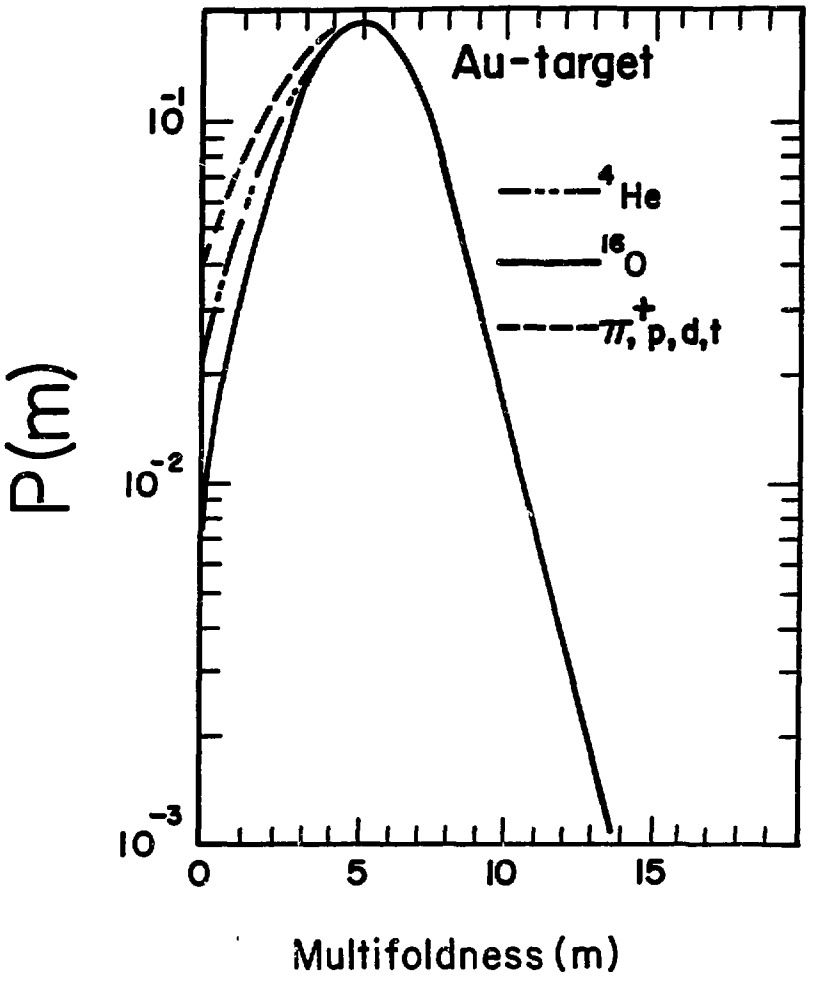
Au-target
^{4}He
^{16}O
π^+, p, d, t
P(m)
10^{-1}
10^{-2}
10^{-3}
0
5
10
15
Multifoldness (m)

Fig. 8

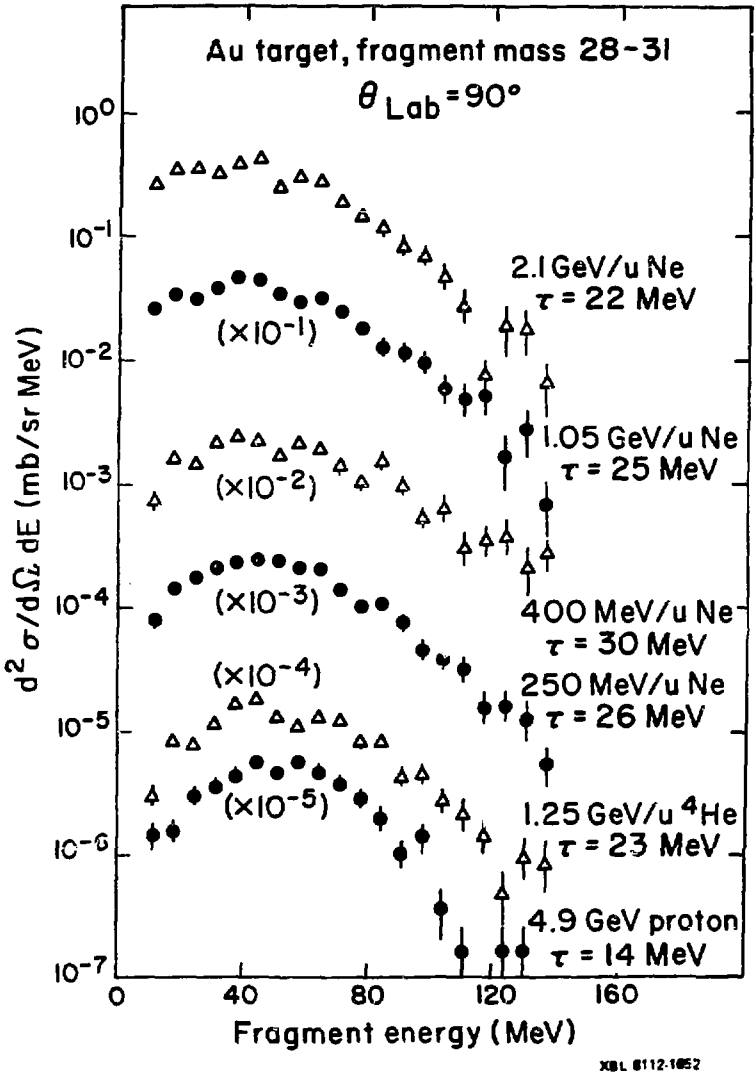

XBL 8112-1852

Fig. 9

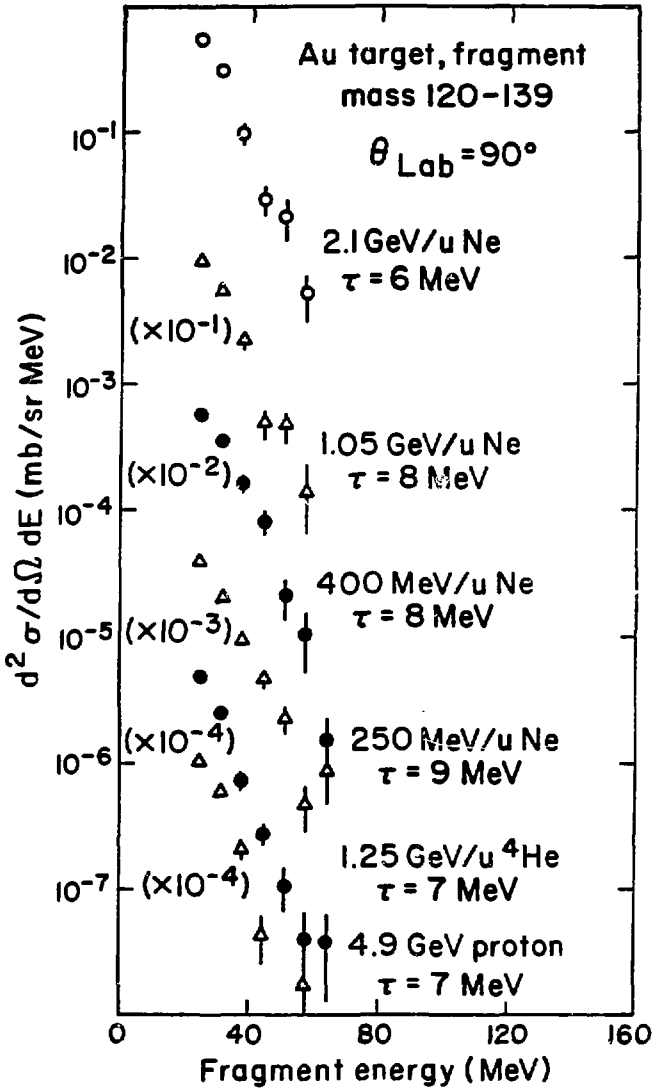

XBL 8112-1651

Fig. 10

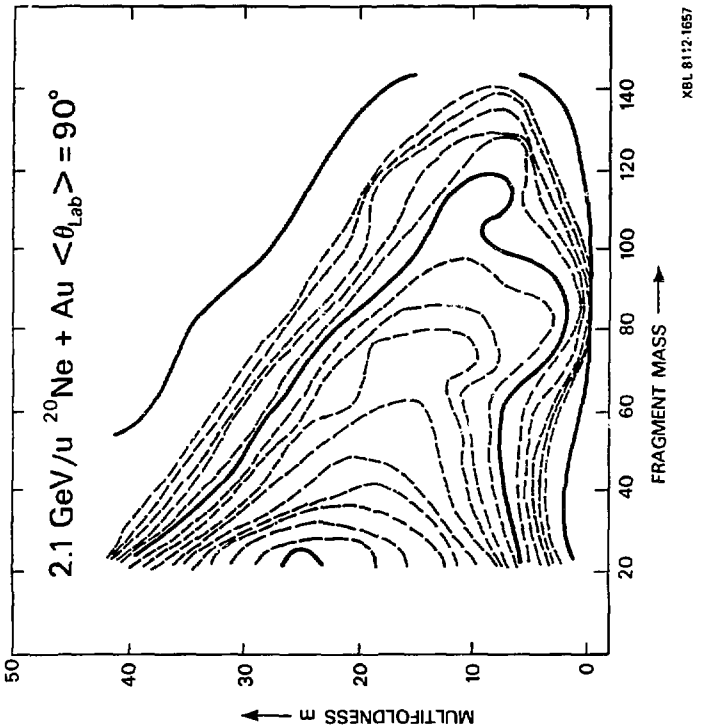
2.1 GeV/u ^{20}Ne + Au $\langle\theta_{Lab}\rangle = 90°$
MULTIFOLDNESS m
FRAGMENT MASS
0
10
20
30
40
50
20
40
60
80
100
120
140
XBL 8112-1657

Fig. 11

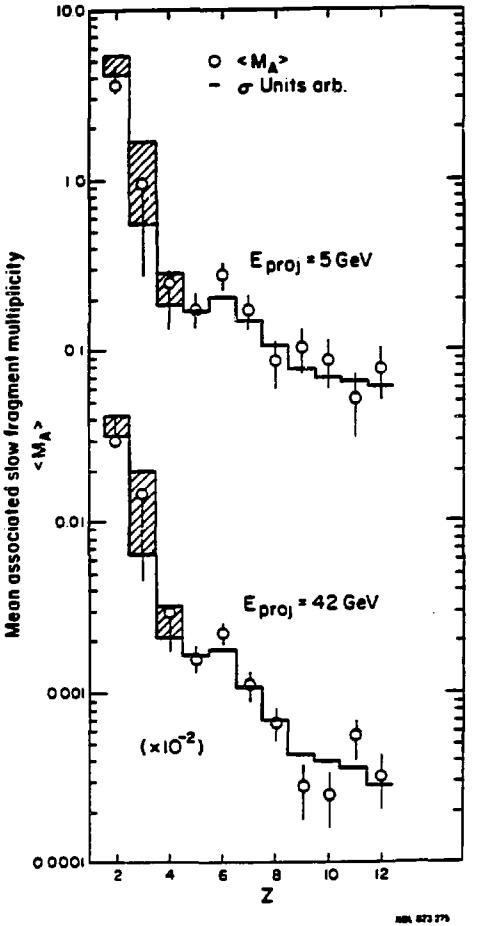
100
10
0.1
0.01
0.001
0.0001
2
4
6
8
10
12
Z
Mean associated slow fragment multiplicity
<M_A>
○ <M_A>
– σ Units arb.
E_proj = 5 GeV
E_proj = 42 GeV
(×10^-2)

Fig. 12

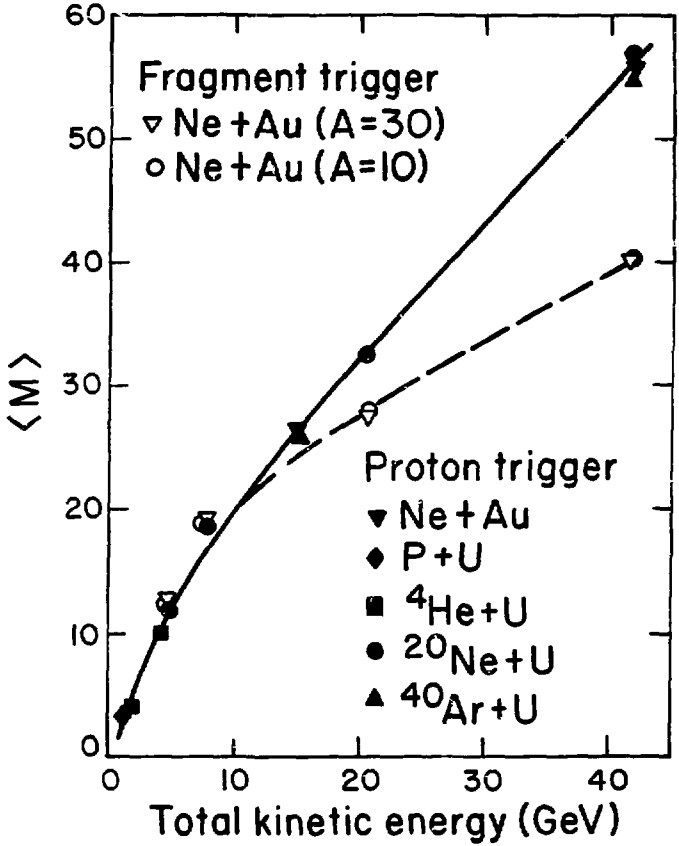

XBL XBL 823-249

Fig. 13

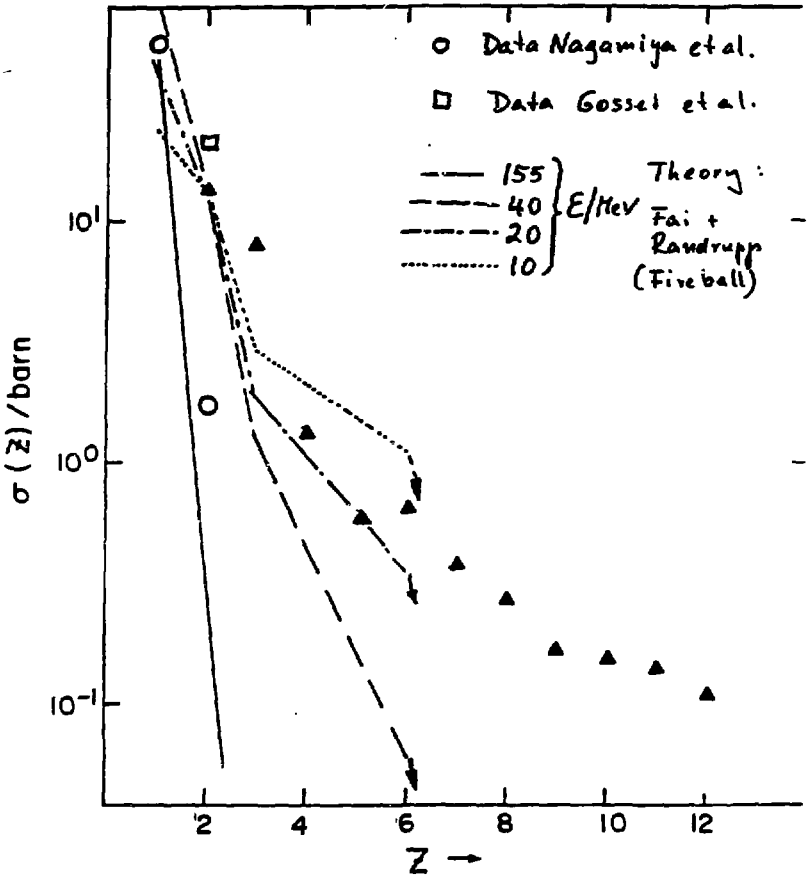
Data Nagamiya et al.
Data Gosset et al.
155
40
20
10
E/MeV
Theory :
Fai + Randrupp (Fireball)
10^1
10^0
10^{-1}
σ (Z) / barn
2
4
6
8
10
12
Z →

Fig. 14

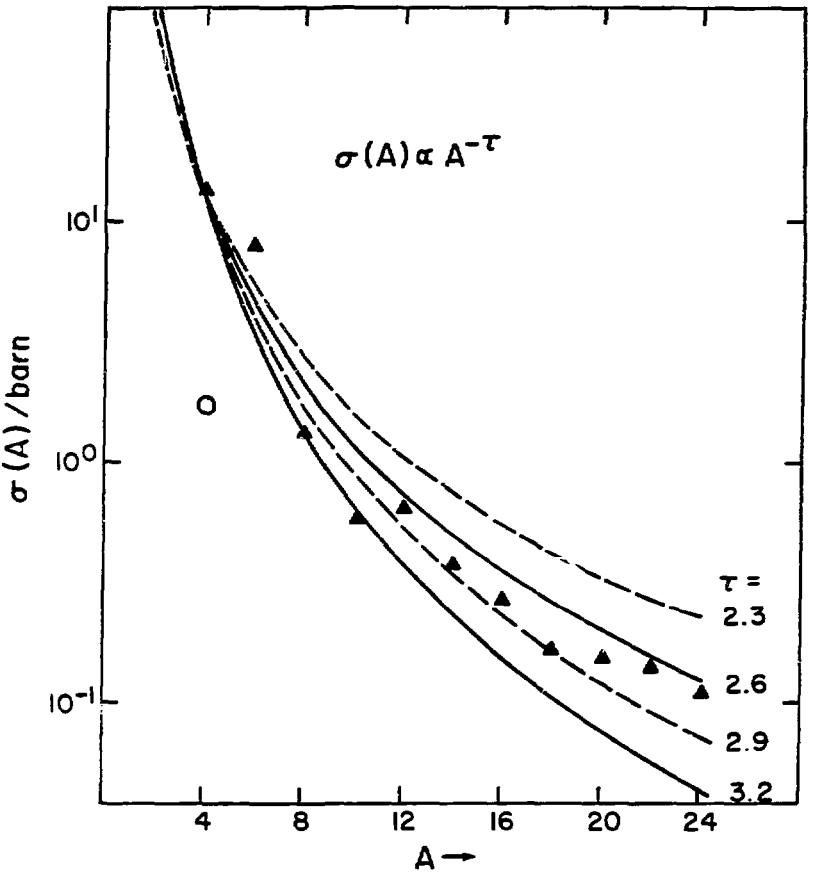

XBL 823-280

Fig. 15

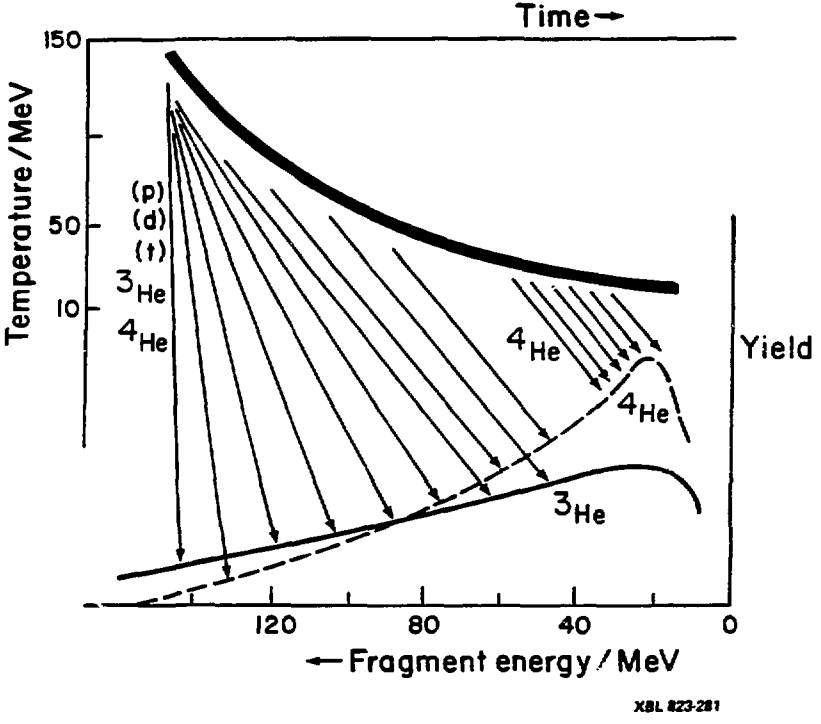
Time→
150
50
10
Temperature / MeV
(p)
(d)
(t)
3He
4He
4He
4He
3He
Yield
120
80
40
0
← Fragment energy / MeV
XBL 823-281

Fig. 16